



Modeling forest biomass using Very-High-Resolution data - Combining textural, spectral and photogrammetric predictors derived from spaceborne stereo images

Joachim Maack^{1*}, Teja Kattenborn², Fabian Ewald Fassnacht², Fabian Enble¹,
Jaime Hernández³, Patricio Corvalán³ and Barbara Koch¹

¹University of Freiburg, Chair of Remote Sensing and Landscape Information Systems (FeLis), Germany

²Institute for Geography and Geoecology (IfGG), Karlsruhe Institute of Technology (KIT), Germany

³Laboratorio de Geomática y Ecología del Paisaje, Universidad de Chile, Santiago de Chile

*Corresponding author, e-mail address: joachim.maack@felis.uni-freiburg.de

Abstract

We used spectral, textural and photogrammetric information from very-high resolution (VHR) stereo satellite data (Pléiades and WorldView-2) to estimate forest biomass across two test sites located in Chile and Germany. We compared Random Forest model performances of different predictor sets (spectral, textural, and photogrammetric), forest inventory designs and filter sizes (texture information). Best model performances were obtained with photogrammetric combined with either textural or spectral information and smaller, but more field plots. Stereo-VHR images showed a great potential for canopy height model (CHM) generation and could be an adequate alternative to LiDAR and InSAR techniques.

Keywords: Biomass modelling, WorldView-2, Pléiades, random forest, photogrammetry, canopy height models.

Introduction

Woody biomass is one of the major resources for an emerging sustainable bio-economy [Becker et al., 2009]. Therefore, sustainable forest ecosystem management as well as climate protection mechanisms such as Reducing Emissions from Deforestation and Degradation (REDD+) depend on reliable and concise information about the temporal and spatial distribution of forest biomass. Furthermore, accurate forest biomass estimations are needed to evaluate the potential of forest ecosystem services (e.g. erosion control). In the field of remote sensing, various sensors and approaches have been evaluated to model aboveground biomass [Lu, 2006; Koch, 2010]. Most frequent approaches used remote sensing predictors in combination with in situ measurements to train parametric or non-parametric regression models [Fassnacht et al., 2014].

According to the close association between tree height and wood volume, canopy height models featured a high explanatory power for forest biomass estimations [Koch, 2010].

Hence, on a local to regional scale the most accurate results were generally obtained using data from airborne Light Detection And Ranging (LiDAR) systems [Lefsky et al., 2002; Clark et al., 2011; Næsset et al., 2011]. However, airborne missions are generally too expensive for national and multi-temporal forest resource assessments.

If a priori a Digital Terrain Model (DTM) is available, Very High-Resolution (VHR) stereo pairs (e.g. derived from GeoEye-1, Ikonos, Pléiades or WorldView-2) enable the generation of accurate Canopy Height Models (CHM) [Huaguo and Biao, 2011; Neigh et al., 2014]. The potential of spaceborne photogrammetric CHMs for the estimation of forest biomass or timber stock has been demonstrated in several studies [e.g. St-Onge et al., 2008; Straub et al., 2013; Kattenborn et al., 2015].

Besides the CHM information, VHR stereo pairs can be used to extract spectral-based predictors. Predictors derived from multispectral sensors achieved moderate success for estimating forest biomass [Nelson et al., 2000; Lu et al., 2005; Anaya et al., 2009]. Especially in dense forest stands with closed and multi-layered canopies, the spectral signal saturates at high biomass values. However, spectral reflectance yields information on tree species and condition [Carleer and Wolf, 2004; Waser et al., 2014]. Particularly in mixed forests, the latter might be a complement to CHM information, since forest biomass can be expressed as a function of heights and diameters of trees and their species dependent wood properties.

An additional predictor type for forest biomass is given by texture information, i.e. parameters that spatially characterize the reflectance patterns. Texture parameters can contain information on canopy closure and shape. Few studies demonstrated the predictive performance of textural predictors as well as their combination with spectral predictors for aboveground biomass modeling [Ozdemir and Karnieli, 2011; Eckert, 2012; Shamsoddini et al., 2013].

Accordingly, stereo-VHR acquisitions allow for extracting different biomass related predictor types, whereas data harmonization and -processing efforts as well as acquisition costs are relatively low in comparison to multi-sensor approaches. These, photogrammetric, spectral and texture based predictors inherit different tree and forest stand characteristics. It seems reasonable, that combining all predictor types increases the accuracy of biomass estimations. To validate this hypothesis we compare biomass estimates based on the single predictor types as well as their combination for a temperate and a sub-mediterranean temperate forest site. According to our literature research the majority of studies related to biomass and remote sensing does not account for site-specific properties, e.g. topographic biomass patterns, within their accuracy assessments. Hence, we check the robustness of our biomass models with regard to our site-specific characteristics i.e. mountainous terrain and tree species composition. As indicated by previous studies [Zolkos et al., 2013; Fassnacht et al., 2014], the training of remote sensing based biomass models depends on an adequate field sampling, in terms of size and number of field plots. To evaluate the importance of these properties for VHR data we used two different field sample sets for each site.

Material and Methods

Study Site Karlsruhe, Germany

The first study site is located near Karlsruhe (49°03'37"N, 8°24'09"E to 49°01'15"N, 8°25'49"E), Germany (Fig.1) and covers an area of approximately 900 ha. The site is representative for managed European temperate forests. The area is mainly covered by Scots pine (*Pinus sylvestris*), European beech (*Fagus sylvatica*), sessile oak (*Quercus petraea*)

red oak (*Quercus rubra*), wild cherry (*Prunus avium*) and hornbeam (*Carpinus betulus*). Forest compartments embrace pure and mixed stands of different age. The terrain is flat and ranges from altitudes of 109 m to 114 m above sea level. Field data was collected during a three-week field campaign between mid-August and the beginning of September 2013.

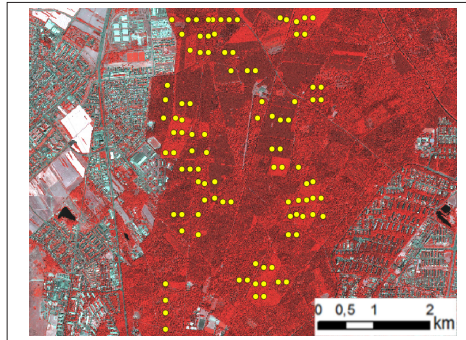


Figure 1 - False color infrared image (WorldView-2) and cluster locations (yellow) of the study site Karlsruhe, Germany. Each cluster contains three field plots.

Study Site Monte Oscuro, Chile

The second test site is located in the Maule region of central Chile ($35^{\circ}7'0''S$, $70^{\circ}55'26''E$) and extends over an area of 1260 ha. The dominant tree species is Roble beech (*Nothofagus oblique* (Mirb.) Oerst.). Further species are Mañío de hojas largas (*Podocarpussalignus* D. Don), Naranjillo (*Citronellamucronata* (Ruiz&Pav.) D. Don), Piñol (*Lomatiadentata* (Ruiz&Pavón) R. Br.), Peumo (*Cryptocaryaalba* (Mol.) Looser) and Olivillo (*Aextoxicon punctatum* Ruiz&Pavón). Due to the very low management impact the site is in a quasi-natural state and can be considered as a secondary growth native forest. The terrain is rough and ranges from altitudes of 700 m to 1400 m above sea level. The forest cover is characterized by a high horizontal and vertical structural diversity. Field data were collected during a field campaign in Chilean summer between January and March 2013.

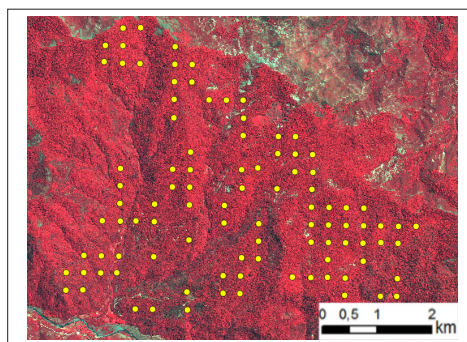


Figure 2 - False color infrared image (Pléiades) and cluster locations (yellow) of the study site Monte Oscuro, Chile. Each cluster contains three field plots.

Field Sampling and Reference Data Calculation

For both test sites cluster locations were pre-selected based on inventory maps to ensure that reference data of all major forest types and age classes were sampled ($n=98$ for Chile, $n=101$ for Germany, see Fig. 1 and Fig. 2). Each cluster consists of 3 satellite field plots. The inventory design of the field plots followed an approach of concentric rings with radii of 2 m, 3 m, 6 m and 12 m. In each of these rings trees with a Diameter at Breast Height (DBH) exceeding 7 cm, 10 cm, 15 cm and 30 cm, respectively were measured. Measurements included the DBH and the species for all trees. For a subset of trees in each field plot, height was measured with a Vertex Hypsometer. The satellite plots represent field measurements with very close spatial association, assuming that forest characteristics vary only marginal between them. By applying species-specific allometric equations [Zianis et al., 2005; Zell, 2008; Annighöfer et al., 2012] above ground biomass was calculated for each individual tree, based on the DBH and for some species on DBH and tree height. Finally, the single tree biomass values were converted to t/ha by using expansion factors. Expansion factors for each concentric ring were defined as 1 ha / area of ring with radius x. Summaries of the biomass reference data are given in Table 1 and Table 2. Further details regarding the test sites, sampling and biomass calculations are given in Fassnacht et al. [2014] and Corvalán et al. [2014].

Table 1 - Statistical summary of the field data sets in Karlsruhe, Germany. All values except count are given in t/ha.

	Count	Min.	1 st Qu.	Median	Mean	3 rd Qu.	Max.	Sdev.	Range
Plot	303	54.6	145.6	185.7	196.1	239.8	444.2	86.17	389.6
Cluster	101	100.9	169.6	189.3	196.1	227.6	302.0	68.88	201.1

Table 2 - Statistical summary of the field data sets in Monte Oscuro, Chile. All values except count are given in t/ha.

	Count	Min.	1 st Qu.	Median	Mean	3 rd Qu.	Max.	Sdev.	Range
Plot	294	33.07	97.5	146.2	162.7	204.3	439.8	65.13	406.7
Cluster	98	37.9	120.1	153.1	166.9	207.7	365.1	51.22	327.1

Remote Sensing Feature Space Setup

The photogrammetric CHM generation was based on two WorldView-2 scenes, acquired on 8th and 23th of June 2013 (study site Karlsruhe) and two Pléiades scenes, acquired on 25th of January 2013 (study site Monte Oscuro). The ERDAS IMAGINE Photogrammetry 2014 module (Leica Geosystems, Atlanta, Georgia, USA) was used to produce photogrammetric point clouds. A subsequent DSM interpolation was performed using TreesVis 0.86 [Weinacker et al., 2004] with a pixel size of 1 m. On the basis of the Pléiades and the WorldView-2 DSMs the respective CHMs were computed for both test sites by subtracting airborne LiDAR DTMs. LiDAR data for Karlsruhe was collected in 2007 and in 2011 for Monte Oscuro with a LMS-Q560 laser scanner (16 points/m²). Detailed information on the LiDAR acquisitions is given in Fassnacht et al. [2014].

Preprocessing of the spectral bands was carried out in ENVI (Exelis Visual Information

Solutions, Boulder, Colorado, USA). Digital numbers were converted to top-of-the-atmosphere reflectance using absolute radiometric calibration factors provided by the satellite data providers and subsequent atmospheric corrections (FLAASH).

We used all available bands of both Pléiades (4 bands) and WorldView-2 (8 bands), so that both predictor sets are derived from an almost equal spectral range (approx. 400 - 1000 nm). The extracted textural information is based on a co-occurrence analysis of all spectral bands, including Mean, Variance, Homogeneity, Contrast, Dissimilarity, Entropy, Second Moment and Correlation. We generated three different texture predictor sets for both test sites in order to identify potential effects of different window sizes (3×3, 5×5, 7×7).

To improve the data handling and analysis we performed a PCA to decompose the spectral as well as the textural feature space into sequences of principle components (PC). These components can be interpreted as particular surface features, which concentrate similar information derived from multiple input features into single PCs. Especially with regard to the number of textural predictors we assume that a PCA minimizes cross-correlation and thereby increases the signal/noise ratio in the feature space. The first component of the PCA generally represents the dominant signal of the input data while the following components contain less frequent information and more noise [Eastman and Fulk, 1993]. Nevertheless, not only the first PC should be taken in consideration [Cheriyadat and Bruce, 2003] as the dominant signal may not be related to the variable of interest. For example for forest biomass estimation, the dominant signal could be the difference between urban and natural areas, however, the spectral information that is relevant for estimating biomass would rather be the more subtle spectral information related to tree species which are stored in one of the later PCs. Thus, we extracted multiple PCs to cover the majority of information inherited by the spectral and textural data. Summarized information on the satellite data and the produced predictor sets is given in Table 3.

Table 3 - Specifications of the sensors used and the derived predictors.

Sensor	WorldView-2	Pléiades
Acquisition date	08-06-13 and 23-06-13	25-01-13
Spatial resolution	Pan. 46 cm Multi. 185 cm	Pan. 50 cm Multi. 200 cm
Spectral resolution	8 bands (400 -1040 nm)	4 bands (430-950nm)
Spectral predictors (S)	PCA 1-4 (of 8)	PCA 1-3 (of 4)
Texture predictors (T)	PCA 1-10/64 (Mean, Variance, Homogeneity, Contrast, Dissimilarity, Entropy, Second Moment, Correlation)	PCA 1-10/32 (Mean, Variance, Homogeneity, Contrast, Dissimilarity, Entropy, Second Moment, Correlation)
Photogrammetric predictors (P)	CHM mean height, CHM standard deviation, CHM range	CHM mean height, CHM standard deviation, CHM range

The spectral, textural and photogrammetric feature space was extracted using the entire extend of the field plots (radius 12 m) using the mean values of all pixels covered by the same polygon.

Predictor Selection and Model Validation

We applied multiple model setups in order to investigate whether a combination of the predictor types increases the accuracy of the biomass estimation. The analysis was performed with R [R Core Team, 2009]. Models were applied using solely spectral (S), textural (T) or photogrammetric (P) predictors as well as combinations of them, i.e. S+T, S+P, T+P and S+T+P. We assessed the cross correlation between all predictor variables by calculating Pearson's r for each model and the respective predictor combination. In case the correlation between two variables was greater than 0.7 we removed the variable, which had the overall highest correlation among the entire predictor set.

As regression model algorithm the Random Forest algorithm implemented in R (package `randomForest` [Liaw and Wiener, 2002]) was chosen. An advantage of non-parametric regression models is that these are often less affected by non-normal data distributions. The conceptual design of the Random Forest leads to a high flexibility and robustness in regard to outliers and noise [Breiman, 2001]. The Random Forest algorithm is also known to be relatively insensitive to the 'Hughes effect', i.e. small sample sizes in combination with a high dimensional feature space, i.e. predictor variables. Accordingly, the Random Forest model was already successfully applied in the field of Remote Sensing [Latifi et al., 2010; Garcia-Gutierrez et al., 2011; Fassnacht et al., 2014; Kattenborn et al., 2015]. For model validation the .632 Bootstrap was applied [Efron and Tibshirani, 1997] to calculate RMSE and normalized root mean square error (NRMSE). The 632 and 632+ Method works best in comparison to other cross validation algorithms with rather weak signal-to-noise ratio and rather small sample sizes [Borra and Ciaccio, 2010].

For each predictor combination a recursive model selection was applied to ensure that only predictors were selected that decrease the overall model uncertainties. Accordingly, in each run one predictor was removed and the RMSE was assessed. If the RMSE increased the respective predictor was excluded from the final predictor set. Within each step 500 repetitions were performed. This procedure was continued until convergence of the RMSE value. We calculated the normalized root mean square error ($\text{NRMSE} = \text{RMSE} / (y_{\max} - y_{\min})$) to allow for a comparison between plot- and cluster-based model results. Where y_{\max} and y_{\min} represent the maximum and minimum observed biomass values respectively.

Results

Our results depend on test sites representing two differently managed forests. However, we aim for a general performance test of this approach rather than on sensor or study site comparison.

Texture Window size

For both data sets the described model validation was performed for each texture predictor set. The different window sizes were compared using the S+T+P predictor combination. In general, a window size of 3 pixels resulted in most accurate biomass estimates (Fig. 3). For both data sets the differences in NRMSE were marginal (max 0.04% Karlsruhe, 0.63% Monte Oscuro). There is only a very slight tendency that fine structural details provide more information for biomass estimation.

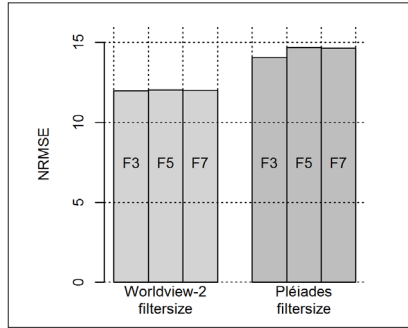


Figure 3 - Model results using the different filter sizes and a combination of all predictor types (S+T+P).

Feature Space Reduction

We applied a principal component analysis (PCA) to address possible intercorrelations among the predictors and to separate signal from noise. The PCA accumulates the dominant information in the first few PCs. Thus, by excluding the last few PC the feature space can be shrunk efficiently without losing relevant information. This was confirmed by the recursive model selection, which excluded only 2 variables for the final Karlsruhe- and none for the Monte Oscuro-dataset. Thus, we prevented the model from overfitting by using fewer but highly optimized predictors.

Predictor Performance

In Karlsruhe the differences in model performance (NRMSE) between P (12.91 %) and S (12.93 %) or T (12.46 %) show no clear trend. We assume that this is an effect of the relatively distinct patterns in species composition and treatment. For this data set the predictor combinations S+P and S+T+P achieved the best results. Figure 4 shows the regression line and the associated results for each field measurement and its related biomass estimation for all tested predictor type combinations. In addition, the uncertainties of the estimation are indicated by 95% confidence intervals derived from the 500 bootstrap runs.

Table 4 - Model results for test site Karlsruhe, Germany.

Site: Karlsruhe, Germany	Plot		Cluster	
	RMSE [t/ha]	NRMSE [%]	RMSE [t/ha]	NRMSE [%]
Spectral	50.39	12.93	41.45	20.61
Texture	48.55	12.46	39.49	19.64
Photogrammetric	50.28	12.91	41.74	20.76
Spectral + Photogrammetric	46.60	11.96	39.11	19.45
Spectral + Texture	48.23	12.38	39.61	19.70
Texture + Photogrammetric	46.99	12.06	38.96	19.37
Spectral +Texture + Photogrammetric	46.67	11.97	38.98	19.38
Mean	48.24	12.38	39.91	19.84

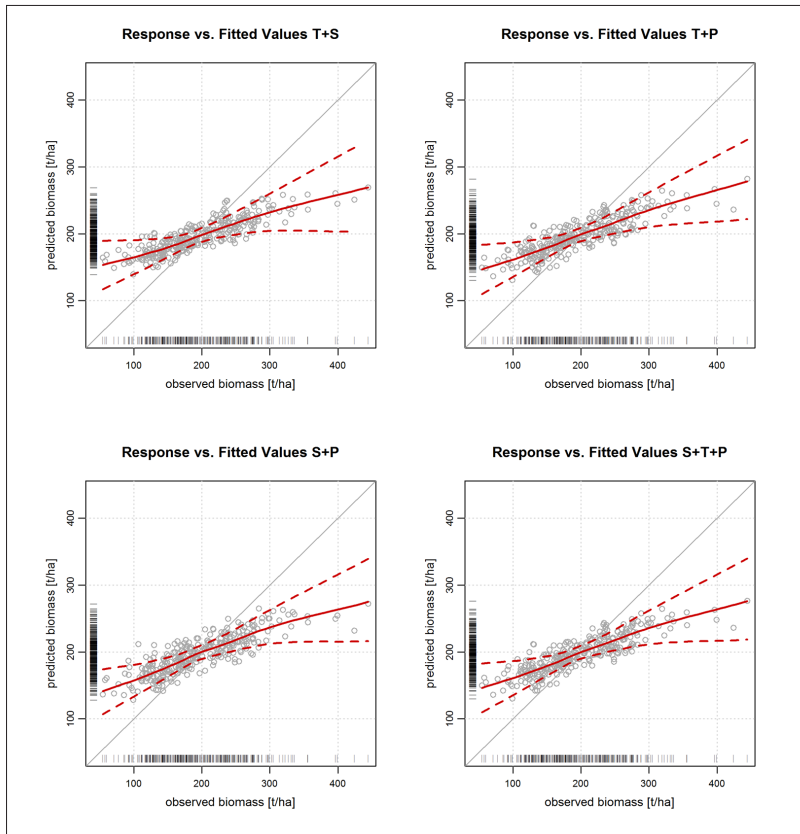


Figure 4 - Model fits (plot-based) for the test site Karlsruhe, Germany. Response (x-axis) and Predicted (y-axis) biomass values based on the RF using varying combinations of T+S+P; solid red lines are local regression fits of the averaged 500 predictions per plot (grey circles, $n = 303$); dashed red lines, i.e. standard deviation, indicate model uncertainties; vertical bars represent the field observations.

There is almost no difference between the NRMSE for S+P (11.96) compared to T+P (12.06%) for the Karlsruhe test site.

In Monte Oscuro, models that incorporated the photogrammetric predictors (P), i.e. absolute canopy height values and standard deviation, achieved the highest model performance (Tabs. 4 and 5). This applies for photogrammetric predictors alone as well as their combination with other predictors (S+T, T+P, S+T+P). Especially in comparison to models based on S, T or S+T the relatively high explanatory power of the P predictors became apparent. Forest height information (P) constitutes the best predictor (NRMSE 14.57 %), whereas the predictive performance of S (16.41 %) and T (15.61 %) is lower. These performances are in line with other studies that combined CHM products and spectral information [e.g. Anderson et al., 2008; Fassnacht et al., 2014; Kattenborn et al., 2015]. Combining all predictor types (S+T+P) gives the best model results (14.06 %). However, predictive accuracy and model fit is only slightly increased compared to the combinations S+P (14.41 %) or T+P (14.13 %) (Fig. 5).

Table 5 - Model results for test site Monte Oscuro, Chile.

Site: Monte Oscuro, Chile	Plot		Cluster	
Predictor set	RMSE [t/ha]	NRMSE [%]	RMSE [t/ha]	NRMSE [%]
Spectral	66.73	16.41	55.12	16.85
Texture	63.49	15.61	51.24	15.66
Photogrammetric	59.27	14.57	53.17	16.25
Spectral + Photogrammetric	58.61	14.41	48.85	14.93
Spectral + Texture	63.09	15.51	51.48	15.74
Texture + Photogrammetric	57.47	14.13	48.51	14.83
Spectral +Texture + Photogrammetric	57.17	14.06	47.71	14.59
Mean	60.83	14.96	50.87	15.55

Combining T+P (14.13 %) on the Monte Oscuro test site resulted in more accurate estimates than using S+P (14.41 %). As a result of the natural regeneration in this area the species composition is rather homogenous than patchy. We assume that total biomass values on this test site do not largely depend on the species composition but on local structural characteristics. Hence, textural predictors might inherit a higher explanatory power in this type of forests.

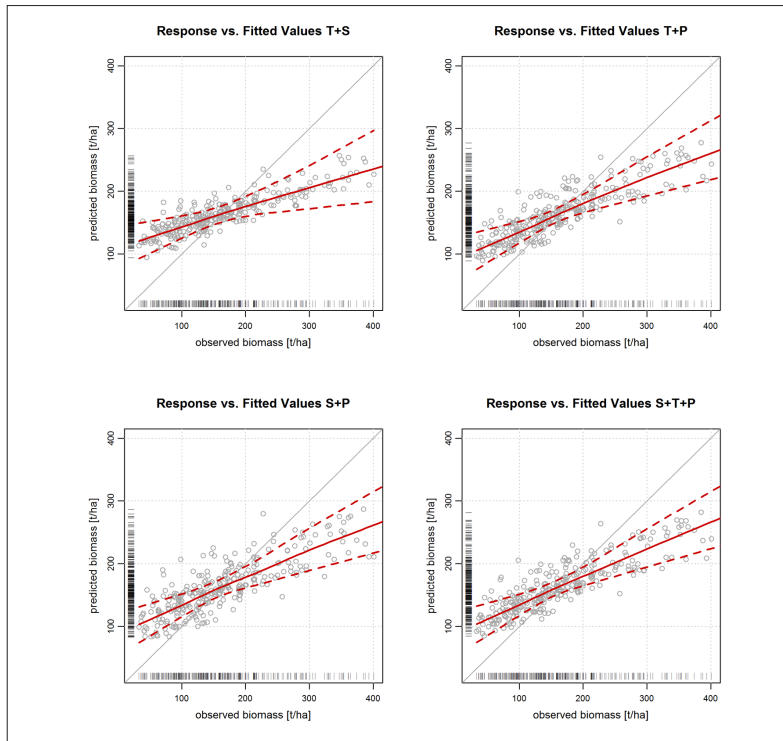


Figure 5 - Model fits (plot-based) for the test site Monte Oscuro, Chile. Response (x-axis) and Predicted (y-axis) biomass values based on the RF using varying combinations of T+S+P; solid red lines are local regression fits of the averaged 500 predictions per plot (grey circles, $n = 294$); dashed red lines, i.e. standard deviation, indicate model uncertainties; vertical bars represent the field observations.

Plot vs. Cluster Reference Data

Compared to plot-based models the cluster-based models resulted in higher NRMSE for both test sites and all predictor types and combinations (Tabs. 4 and 5). Overall differences in NRMSE values between the two reference data types were smaller in Monte Oscuro. In particular models based on S, P and S+P differed only marginally. Contrary, cluster based models in Karlsruhe resulted in markedly lower model performances (mean NRMSE 19.84) than plot based models (mean NRMSE 12.38).

Site-specific Model Bias Karlsruhe

The two test sites inherit characteristics, which might lead to a bias of the model estimates. The low slope of all regressions (Fig. 4 and 5) clearly indicates a regression dilution. We expected a model bias in Karlsruhe since the site features a high heterogeneity of species composition between the single forest stands. We assumed, that the spectral resolution of WorldView-2 might not allow for accurate tree species related biomass estimations. To investigate this assumption we plotted the model residuals against the coniferous wood ratio (see Fig. 6). However, the results show no clear trend. Thus a model bias related to tree species cannot be confirmed.

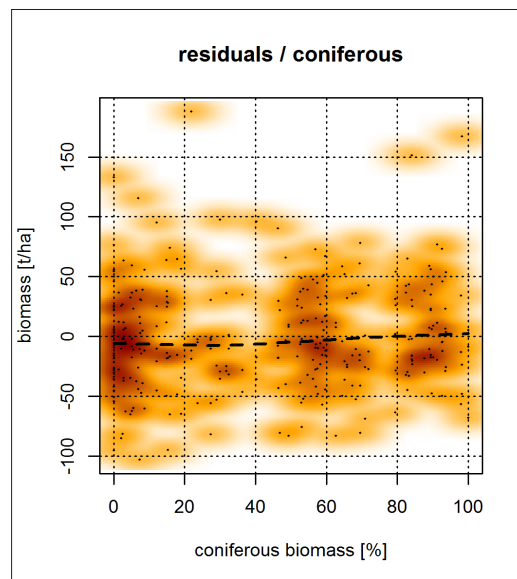


Figure 6 - Proportion of coniferous forest in Karlsruhe, Germany against averaged model residuals of 500 bootstraps.

Site-specific model bias Monte Oscuro

We compared the observed biomass values and the model residuals for Monte Oscuro, in order to check the model robustness or a potential bias with regard to varying terrain elevation. Figure 7 shows the measured biomass values (a) and model residuals (b) respectively (variable type combination S+T+P) plotted against the terrain elevation. The

trend, visualized by a local regression, indicates that lower biomass values are mainly present at rather low (< 900 m) and high (>1300 m) altitude.

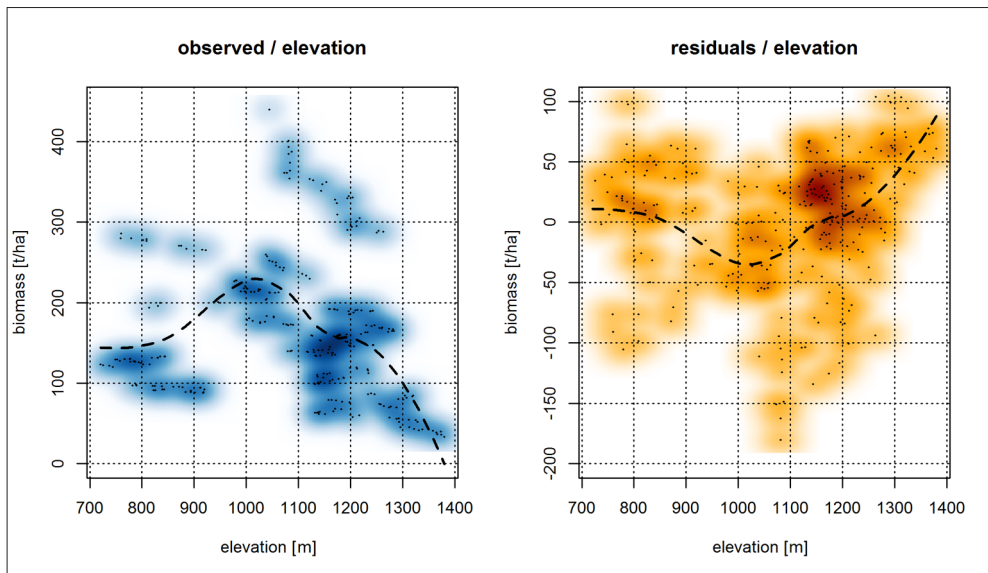


Figure 7 - Elevation derived from a LiDAR DTM in Monte Oscuro against averaged biomass values (left) and model residuals of 500 bootstraps (right).

Discussion

Spectral vs. texture predictors

From the results of both test sites we deduce that S and T inherit very similar information content related to forest biomass. This is also reflected in the low differences in model performance using either S or T or S+T. Regarding an operational application it might be more efficient to combine either S or T with P instead of combining all predictor types. This also enables to keep the model as parsimonious as possible.

The direct comparison between the two sites is limited due to the use of different sensors and site-specific characteristics. However, we assume that the relative comparisons between T and S are robust, as we used similar bands widths to derive the spectral and textural predictors for the respective data set. The increased band number of WorldView-2 might be a potential reason for the higher explanatory power of S in Karlsruhe, and likewise the number of textural bands and therefore information content is increased.

With regard to the explanatory power of spectral and textural predictors further studies have to be conducted to analyze effects of sun and sensor position during image acquisition. Concerning the illumination geometry Eckert [2012] states that the relationship between textural predictors and forest biomass decreases if cast shadows are minimal. We expect an opposite effect for spectral predictors, i.e. a stronger relationship between spectral predictors and forest biomass with minimized cast shadows. Accordingly, such image acquisition related characteristics have to be considered when choosing either spectral or textural predictors.

Plot vs. Cluster Reference Data

The derived clusters represent field samples with a higher sampling area per unit. As discussed by Zolkos et al. [2013] an increased area size for sampling is potentially less prone to errors, e.g. caused by trees with overlapping canopy outside the plot area and general sampling inaccuracy. Furthermore using a greater field sampling area is likely to decrease effects of GPS positioning inaccuracies during field sampling as well as registration errors of the satellite data. However, our results show no improvement using the clustered samples. This is partly in line with a previous study on the test site Karlsruhe [Kattenborn et al., 2015], where clustered samples did improve model performance for a hyperspectral/SAR fusion, but not for a hyperspectral/VHR fusion.

In general, clustering smoothes both response values and remote sensing feature space. Accordingly, the lower model performance of cluster-based models might be attributable to a loss of information due to smoothing. This would also explain the relatively high differences between the plot and cluster approaches in Karlsruhe, where due to the heterogenic forest stands more information is required to accurately model biomass. We therefore assume that especially for areas with distinct forest stands, e.g. in terms of species composition and treatment, increased sample intensity might be a more important factor than sampling area size. This appears to contradict the findings of Zolkos et al. [2013], where the effects of different sample area sizes were compared using the relative standard error (RSE). However, our sampling size for the clustered approach ($n = 98$ for Monte Oscuro, $n = 101$ for Karlsruhe) might not allow for a general statement and has to be validated in further studies.

Model uncertainties

Our model results show relatively large uncertainties and a general overestimation for low biomass values. Accordingly, in Monte Oscuro our biomass estimations in areas with high and low elevations are generally overestimated and characterized by high uncertainties. This is visualized in Figure 8, showing the extrapolated residual/height trend within a part of the Monte Oscuro study area. We assume that lower biomass values at high altitudes are caused by limited water supply. This might be caused by increased transpiration rates due to stronger winds and solar radiation as well as lower water flow accumulation and decreased minimum and mean temperatures. Small biomass values at low altitudes are most likely a result of reduced exposure to sunlight within valleys as well as increased accessibility and corresponding historic deforestation patterns [Corvalán et al., 2014]. The model residuals plotted against the elevation show a very similar trend compared to observed biomass values against elevation. Hence, further bias – not already present within the field observations – cannot be observed. These findings emphasize, also with respect to previous biomass map products, that accuracy assessments of biomass models have to be analyzed in terms of the spatial relationship between field measurements and abiotic factors. Hence, it can be concluded that empirical biomass models applied on regions with high variation in elevation are prone to a systematic bias caused by natural biomass or height gradients. A stratification into elevation classes might theoretically address this issue; but as the intensity of field sampling is limited within most studies, a stratification will also lead to an insufficient number of field samples for model calibration [Lu, 2006]. Further trends might be present due to effects of terrain exposition and slope, which will be assessed in future work.

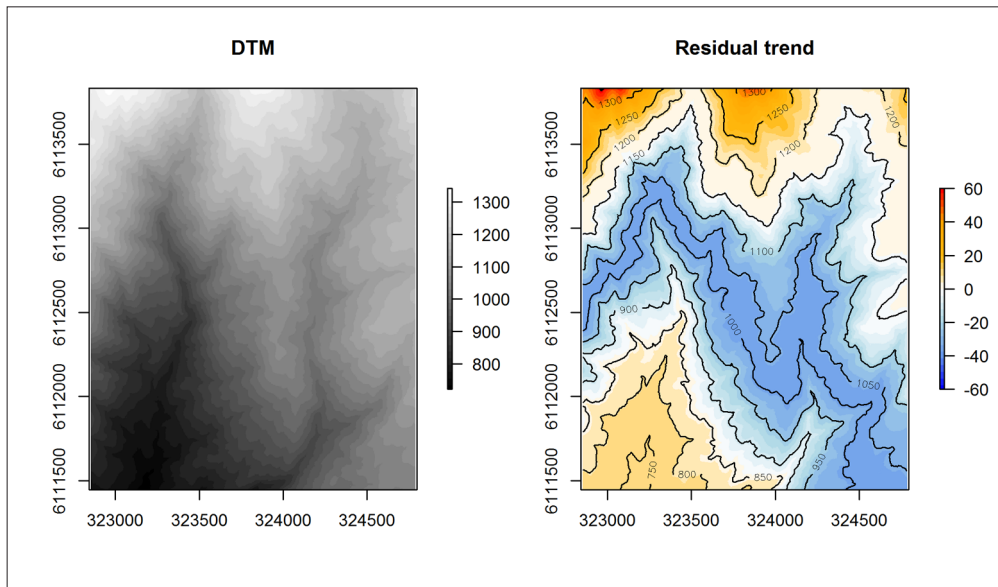


Figure 8 - Contour lines and extrapolated trend of residuals and height (right) applied on the LiDAR DTM (left) of Monte Oscuro.

Alternatives to LiDAR DTM?

Within the presented methodology a LiDAR-based DTM was used for the generation of the CHM. LiDAR surveys have already been accomplished for some areas of the globe. In regions without LiDAR data coverage long wavelength, i.e. L-band or P-band, SAR data might feature an alternative to estimate absolute canopy heights [Andersen et al., 2005; Balzter et al., 2007]. In areas with frequent presence of canopy gaps and rather smooth terrain the photogrammetric point cloud of the VHR data itself could potentially be utilized to interpolate a DTM. However, such alternatives have to be evaluated in future studies.

Conclusion

We examined if a combination of VHR-based photogrammetric, spectral and texture predictors increase the accuracy of forest biomass estimations in comparison to using solely one type of predictors. Therefore, we applied multiple models with different predictor combinations. The results on the two test sites showed similar trends, although two different VHR sensors were used.

As expected, including photogrammetric predictors, i.e. information on canopy height, resulted in overall highest model performances. The results of both test sites show that combining all predictor types only slightly increases the accuracy of the biomass estimations. Thus, related to biomass spectral and textural predictors inherit relatively similar information. With respect to an operational application we recommend to combine either spectral or texture with photogrammetric predictors. Whether to use texture or spectral predictors depends on the geometric illumination properties of the scene and the forest characteristics of the site.

The implemented predictor selection procedure showed that feature space decomposition

(PCA) minimizes predictor inter-correlation and aggregates information content of the respective predictor type. Our results show that within our study sites field sampling intensity is a more important factor for VHR-based biomass estimations than area size of single field samples.

We observed a systematic bias within our biomass models, caused by a correlation between biomass field measurements and terrain elevation. We therefore highly recommend analyzing biomass measurements with regard to systematic effects, caused by abiotic factors, such as elevation and exposition.

Acknowledgments

The study was partly funded by the German National Space Agency DLR (Deutsches Zentrum für Luft- und Raumfahrt e.V.) on behalf of the German Federal Ministry of Economy and Technology on the basis of a decision by the German Bundestag. Support code: 50EE1265. Further funding was received within the BIOCOSA project (SA - Code: 208-7321). We would also like to acknowledge the landowners of the Monto Oscuro site for supporting the field data acquisition. We are thankful to Pléiades Users Group (Astrium) for the provision of the Pleiades imagery which have been delivered to and processed at the Laboratorio de Geomática y Ecología del Paisaje GEP, Universidad de Chile, Chile.

References

- Anaya J.A., Chuvieco E., Palacios-Orueta A. (2009) - *Aboveground biomass assessment in Colombia: A remote sensing approach*. Forest Ecology and Management, 257 (4): 1237-1246. doi: <http://dx.doi.org/10.1016/j.foreco.2008.11.016>.
- Andersen H.E., Reutebuch S.E., McGaughey R.J. (2005) - *Accuracy of an IFSAR-derived digital terrain model under a conifer forest canopy*. Canadian Journal of Remote Sensing, 31 (4): 283-288. doi: <http://dx.doi.org/10.5589/m05-016>.
- Anderson J.E., Plourde L.C., Martin M.E., Braswell B.H., Smith M.L., Dubayah R.O., Hofton M.A., Blair J.B. (2008) - *Integrating waveform LiDAR with hyperspectral imagery for inventory of a northern temperate forest*. Remote Sensing Environment, 112: 1856-1870. doi: <http://dx.doi.org/10.1016/j.rse.2007.09.009>.
- Annighöfer P., Mölder I., Zerbe S., Kawaletz H., Terwei A., Ammer C. (2012) - *Biomass functions for the two alien tree species Prunus serotina Ehrh. and Robinia pseudoacacia L. in floodplain forests of Northern Italy*. European Journal of Forest Research, 131 (5): 1619-1635. doi: <http://dx.doi.org/10.1007/s10342-012-0629-2>.
- Balster H., Rowland C.S., Saich P. (2007) - *Forest canopy height and carbon estimation at Monks Wood National Nature Reserve, UK, using dual-wavelength SAR interferometry*. Remote Sensing of Environment, 108 (3): 224-239. doi: <http://dx.doi.org/10.1016/j.rse.2006.11.014>.
- Becker D.R., Skog K., Hellman A., Halvorsen K.E., Mace T. (2009) - *An outlook for sustainable forest bioenergy production in the Lake States*. Energy Policy, 37 (12): 5687-5693. doi: <http://dx.doi.org/10.1016/j.enpol.2009.08.033>.
- Borra S., Di Ciaccio A. (2010) - *Measuring the prediction error: A comparison of cross-validation, bootstrap and covariance penalty methods*. Computational Statistics & Data Analysis, 54 (12): 2976-2989 doi: <http://dx.doi.org/10.1016/j.csda.2010.03.004>.

- Breiman L. (2001) - *Random Forests*. Machine Learning, 45 (1): 5-32. doi: <http://dx.doi.org/10.1023/A:1010933404324>.
- Carleer A., Wolff E. (2004) - *Exploitation of very high resolution satellite data for tree species identification*. Photogrammetric Engineering & Remote Sensing, 70 (1): 135-140. doi: <http://dx.doi.org/10.14358/PERS.70.1.135>.
- Cheriyadat A., Bruce L.M. (2003) - *Why principal component analysis is not an appropriate feature extraction method for hyperspectral data*. Proceedings of IEEE International Geoscience and Remote Sensing Symposium, 6: 3420-3422. doi: <http://dx.doi.org/10.1109/IGARSS.2003.1294808>.
- Clark M.L., Roberts D.A., Ewel J.J., Clark D.B. (2011) - *Estimation of tropical rain forest aboveground biomass with small-footprint lidar and hyperspectral sensors*. Remote Sensing of Environment, 115: 2931-2942. doi: <http://dx.doi.org/10.1016/j.rse.2010.08.029>.
- Corvalán P., Galleguillos M., Hernández J. (2014) - *Presencia, abundancia y asociatividad de Citronella mucronata en bosques secundarios de Nothofagus obliqua en la precordillera de Curicó, región del Maule, Chile*. Bosque, 35 (3): 257-479.
- Eastman J.R., Fulk M. (1993) - *Long sequence time series evaluation using standardised principal components*. Photogrammetric Engineering and Remote Sensing, 59: 991-996.
- Eckert S. (2012) - *Improved forest biomass and carbon estimations using texture measures from WorldView-2 satellite data*. Remote sensing, 4 (4): 810-829. doi: <http://dx.doi.org/10.3390/rs4040810>.
- Efron B., Tibshirani R. (1997) - *Improvements on cross-validation: the 632+ bootstrap method*. Journal of the American Statistical Association, 92 (438): 548-560. doi: <http://dx.doi.org/10.1080/01621459.1997.10474007>.
- Fassnacht F.E., Hartig F., Latifi H., Berge, C., Hernández J., Corvalán P., Koch B. (2014) - *Importance of sample size, data type and prediction method for remote sensing-based estimations of aboveground forest biomass*. Remote Sensing of Environment, 154: 102-114. doi: <http://dx.doi.org/10.1016/j.rse.2014.07.028>.
- Garcia-Gutierrez J., Gonzalez-Ferreiro E., Mateos-Garcia D., Riquelme-Santos J.C., Miranda D. (2011) - *A Comparative Study between Two Regression Methods on LiDAR Data: A Case Study*. Proceedings of 6th International Conference on Hybrid Artificial Intelligent Systems, May 23-25, Wroclaw, Poland, (II): 311-318. doi: http://dx.doi.org/10.1007/978-3-642-21222-2_38.
- Huaguo H.U.A.N.G., Biao C. (2011) - *Experiment on extracting forest canopy height from WorldView-2*. In: 8th International Conference on Fuzzy Systems and Knowledge Discovery, 4: 2614-2617. doi: <http://dx.doi.org/10.1109/FSKD.2011.6019949>.
- Kattenborn T., Maack J., Faßnacht F., Enßle F., Ermert J., Koch B. (2015) - *Mapping forest biomass from space—Fusion of hyperspectral EO1-hyperion data and Tandem-X and WorldView-2 canopy height models*. International Journal of Applied Earth Observation and Geoinformation, 35: 359-367. doi: <http://dx.doi.org/10.1016/j.jag.2014.10.008>.
- Koch B. (2010) - *Status and future of laser scanning, synthetic aperture radar and hyperspectral remote sensing data for forest biomass assessment*. ISPRS Journal of Photogrammetry and Remote Sensing, 65: 581-590. doi: <http://dx.doi.org/10.1016/j.isprsjprs.2010.09.001>.
- Latifi H., Nothdurft A., Koch B. (2010) - *Non-parametric prediction and mapping of*

- standing timber volume and biomass in a temperate forest: application of multiple optical/LiDAR-derived predictors.* *Forestry*, 83 (4): 395-407. doi: <http://dx.doi.org/10.1093/forestry/cpq022>.
- Lefsky M.A., Cohen W.B., Harding D.J., Parker G.G., Acker S.A., Gower S.T. (2002) - *Lidar remote sensing of above-ground biomass in three biomes.* *Global Ecology and Biogeography*, 11: 393-399. doi: <http://dx.doi.org/10.1046/j.1466-822x.2002.00303.x>.
- Liaw A., Wiener M. (2002) - *Classification and regression by random Forest.* *R news*, 2 (3): 18-22. doi: <http://dx.doi.org/10.1016/j.rse.2009.01.003>.
- Lu D. (2006) - *The potential and challenge of remote sensing-based biomass estimation.* *International Journal of Remote Sensing*, 27: 1297-1328. doi: <http://dx.doi.org/10.1080/01431160500486732>.
- Lu D., Batistella M., Moran E. (2005) - *Satellite estimation of aboveground biomass and impacts of forest stand structure.* *Photogrammetric Engineering & Remote Sensing*, 71 (8): 967-974. doi: <http://dx.doi.org/10.14358/PERS.71.8.967>.
- Næsset E., Gobakken T., Solberg S., Gregoire T.G., Nelson R., Stahl G., Weydahl D. (2011) - *Model-assisted regional forest biomass estimation using LiDAR and InSAR as auxiliary data: A case study from a boreal forest area.* *Remote Sensing of Environment*, 115: 3599-3614. doi: <http://dx.doi.org/10.1016/j.rse.2011.08.021>.
- Nelson R., Kimes D., Salas W.A. Routhier M. (2000) - *Secondary forest age and tropical forest biomass estimation using thematic mapper imagery.* *Bioscience*, 50: 419-431. doi: [http://dx.doi.org/10.1641/0006-3568\(2000\)050\[0419:SFAATF\]2.0.CO](http://dx.doi.org/10.1641/0006-3568(2000)050[0419:SFAATF]2.0.CO).
- Neigh C.S., Masek J.G., Bourget P., Cook B., Huang C., Rishmawi K., Zhao F. (2014) - *Deciphering the precision of stereo IKONOS canopy height models for US forests with G-LiHT airborne LiDAR.* *Remote Sensing*, 6 (3): 1762-1782. doi: <http://dx.doi.org/10.3390/rs6031762#sthash.Js7cifNh.dpuf>.
- Ozdemir I., Karnieli A. (2011) - *Predicting forest structural parameters using the image texture derived from WorldView-2 multispectral imagery in a dryland forest, Israel.* *International Journal of Applied Earth Observation and Geoinformation*, 13 (5): 701-710. doi: <http://dx.doi.org/10.1016/j.jag.2011.05.006>.
- R Core Team (2009) - *Development Core Team. R: A language and environment for statistical computing.* R Foundation for Statistical Computing, Vienna, Austria. Available on line at: <http://www.R-project.org>.
- Shamsoddini A., Trinder J.C., Turner R. (2013) - *Pine plantation structure mapping using WorldView-2 multispectral image.* *International Journal of Remote Sensing*, 34 (11): 3986-4007. doi: <http://dx.doi.org/10.1080/01431161.2013.772308>.
- St-Onge B., Hu Y., Vega C. (2008) - *Mapping the height and above-ground biomass of a mixed forest using lidar and stereo Ikonos images.* *International Journal of Remote Sensing*, 29 (5): 1277-1294. doi: <http://dx.doi.org/10.1080/01431160701736505>.
- Straub C., Tian J., Seitz R., Reinartz P. (2013) - *Assessment of Cartosat-1 and WorldView-2 stereo imagery in combination with a LiDAR-DTM for timber volume estimation in a highly structured forest in Germany.* *Forestry*, 86 (4): 463-473. doi: <http://dx.doi.org/10.1093/forestry/cpt017>.
- Waser L.T., Küchler M., Jütte K., Stampfer T. (2014) - *Evaluating the Potential of WorldView-2 Data to Classify Tree Species and Different Levels of Ash Mortality.* *Remote Sensing*, 6 (5): 4515-4545. doi: <http://dx.doi.org/10.1093/forestry/cpt01710.3390/rs6054515>.

- Weinacker H., Koch B., Weinacker R. (2004) - *Treesvis-a software system for simultaneous 3d-real-time visualisation of dtm, dsm, laser raw data, multispectral data, simple tree and building models*. International Archives of Photogrammetry, Remote Sensing and Spatial Information Sciences, 36: 90-95. Available on line at: <http://www.isprs.org/proceedings/XXXVI/8-W2/WEINACKER2.pdf>.
- Zell J. (2008) - *Methoden für die Ermittlung, Modellierung und Prognose der Kohlenstoffspeicherung in Wäldern auf Grundlage permanenter Großrauminventuren*. PhD Dissertation, 152. Available on line at: http://www.freidok.uni-freiburg.de/volltexte/5400/pdf/zell_diss.pdf.
- Zianis D., Muukkonen P., Mäkipää R., Mencuccini M. (2005) - *Biomass and Stem Volume Equations for Tree Species in Europe*. Silva Fennica, 4 (63). Available on line at: <http://www.metla.fi/silvafennica/full/smf/smf004.pdf>.
- Zolkos S.G., Goetz S.J., Dubayah R. (2013) - *A meta-analysis of terrestrial aboveground biomass estimation using lidar remote sensing*. Remote Sensing of Environment, 128: 289-298. doi: <http://dx.doi.org/10.1016/j.rse.2012.10.017>.